Available online at www.sciencedirect.com
ScienceDirect
Trans. Nonferrous Met. Soc. China 24(2014) 3103−3110
Transactions of Nonferrous Metals Society of China
www.tnmsc.cn

Deformed microstructure and texture of Ti6Al4V alloy

Liu-qing YANG, Yan-qing YANG

State Key Laboratory of Solidification Processing, School of Materials Science and Engineering, Northwestern Polytechnical University, Xi'an 710072, China

Received 20 November 2013; accepted 11 March 2014

Abstract: Microstructure and texture evolution during hot compression of Ti6Al4V alloy with an initial equiaxed microstructure were studied in the temperature range of 850−930 °C, strain rate range of 0.01−1 s^{-1} and engineering compressive strain of 70%. The results indicate that when temperature is below 900 °C and strain rate is higher than 0.1 s^{-1}, the microstructure is mainly composed of elongated α grains. While deforming at higher temperatures and lower strain rates, dynamic recrystallization takes place. Electron back scattered diffraction (EBSD) result shows that during dynamic recrystallization, subgrain boundaries absorb dislocations and the recrystallized grains with high angle grain boundary form. At 930 °C dynamic recrystallization has basically completed, and needlelike α phase forms after water quenching. Pole figure analysis indicates that compared with the initial specimen, textures below 930 °C are weaker, while at 930 °C they are stronger.

Key words: Ti6Al4V alloy; hot compression; dynamic recrystallization; EBSD; texture

1 Introduction

The thermo-mechanical processing route of an engineering alloy determines the microstructure and crystallographic texture and must be controlled for optimum mechanical properties [1]. Ti6Al4V is a two-phase (α+β) alloy and has been widely used in aerospace and biomedical applications due to its excellent over-all properties. Although slip in the body-centered cubic (BCC) β phase is beneficial to deformation of Ti6Al4V, the content of β phase is low (<10%) [2,3]. The majority of the plastic strain is accommodated by the hexagonal close-packed (HCP) α phase, and texture evolution is not noticeably affected by slip in the β phase, thus the deformation behavior is dominated by α phase with limited slip systems [4−6]. However, during high temperature deformation, especially above 900 °C, β phase increases sharply. Therefore, the effect of β phase can not be ignored.

It is well known that microstructure and mechanical properties of titanium alloy are very sensitive to the thermo-mechanical processing parameters. And microstructure evolution not only influences the flow behavior of materials, but also determines the mechanical properties [7]. Much work has been carried out on the microstructure, texture evolution and deformation mechanisms of Ti6Al4V. The effect of processing parameters, including deformation temperature, strain rate and deformation degree on the microstructure evolution and the microstructure variables (grain size and volume fraction of primary α phase) has been investigated [7]. The results show that the effect of isothermal compression on the microstructure is dependent on deformation temperature. The curves of volume fraction of primary α phase versus strain rate are oscillatory above 950 °C, but below 950 °C the volume fraction decreases. It was discussed how the texture develops during recrystallization of both β and α phases [8]. Highly curved regions of the initially kinked α colonies contain significant orientation rotations. At the beginning of the heat treatment, during globularization, these disappear. This is the mechanism behind texture strengthening during globularization. Microstructure and texture development in as-welded and post weld heat treated lab-scale and full-scale Ti6Al4V linear friction welds have been characterized by electron back scattered diffraction (EBSD) [9]. It was revealed that they have

Foundation item: Projects (51071122, 51271147) supported by the National Natural Science Foundation of China; Project (B08040) supported by Program of Introducing Talents of Discipline to Universities ("111" Project), China
Corresponding author: Yan-qing YANG; Tel: +86-29-88460499; E-mail: yqyang@nwpu.edu.cn
DOI: 10.1016/S1003-6326(14)63448-8

different textures, which is attributed to a difference in the variant selections during $\alpha \rightarrow \beta$ transformation. However, no systematical analysis of the flow behavior, evolution of microstructure and texture under large degree of deformation has been presented in these earlier studies.

In the present work, the microstructure and texture evolution related to the local deformation parameters in the compressed specimens of Ti6Al4V alloy, as well as their flow behavior are systematically discussed. Below 900 °C, microstructure and texture evolution of α phase are mainly concerned, and the effect of β phase is considered above 900 °C.

2 Experimental

The cylindrical Ti6Al4V specimens (Fig. 1(a)) with 12 mm in height and 8 mm in diameter were machined with the axis perpendicular to the pre-forging direction. The prepared specimens were deformed by a Gleeble−3500 thermo-mechanical simulator in the temperature range of 850−930 °C, strain rate range of 0.01−1 s^{-1} and the engineering compressive strains of 70%. The materials display significant oscillatory flow at higher strain rates (≥1.0 s^{-1}) [10]. So, in the present work, the strain rates were under 1 s^{-1}.

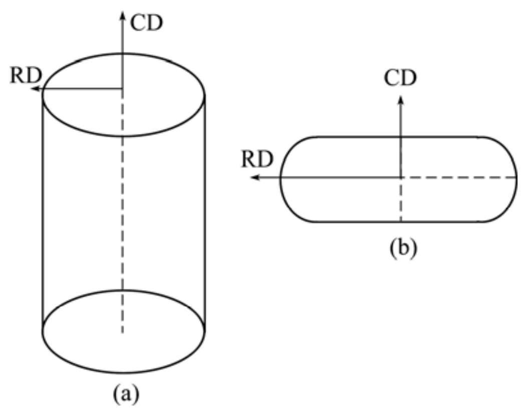

Fig. 1 Sketch maps of cylindrical specimen before (a) and after (b) deformation (Horizontal and vertical directions represent radial and compression directions, RD and CD, respectively)

The specimens were heated to the deformation temperature in air for 200 s to ensure a homogeneous temperature distribution. In order to reduce friction, a tantalum foil with a thickness of 0.1 mm was put between the anvil and the specimen. The stress, temperature and strain rate during deformation were automatically controlled and recorded by the simulator system.

As the ratio of the maximum to the minimum diameter was below 9% after deformation, the influence of friction was not considered [11]. After deformation, the specimens were cooled to room temperature immediately by water quenching. Then the specimens were cut parallel to the loading axis (Fig. 1(b)). The longitudinal sections were mechanically ground and polished prior to observation.

The microstructures of the deformed specimens were examined by a Tescan Mira3 scanning electron microscope (SEM) with Oxford HKL Nordly Max EBSD accessory. EBSD scans were carried out with the specimens tilted 70°, applying an accelerating voltage of 20 kV, and at a working distance of 10 mm. An increment step of 0.4 μm, except specimen with 930 °C, 1 s^{-1}, whose step size was 0.2 μm, was used for the centre sections of the specimens. Recorded Kikuchi patterns were collected at each step increment and indexed using the Oxford Instruments Channel 5 HKL suite of programs.

As severe deformation can cause orientation noise and uncertainty, which could possibly lead to blurring of the grain boundaries, misorientation below 2° was not considered. Grain boundaries with misorientation between 2° and 15° were defined as low angle grain boundaries (LAGBs), and those of misorientation above 15° were defined as high angle grain boundaries (HAGBs) [11]. Of all the EBSD maps presented in this work, the grains were colored according to the standard color codes in the compression direction (CD).

3 Results and discussion

3.1 Microstructure and texture before deformation

The EBSD image of the as-received Ti6Al4V is shown in Fig. 2(a), which presents equiaxed and slightly elongated α grains with an average grain size of 20 μm and intergranular β phase. The color codes in Fig. 2(b) give the crystallographic direction of each grain pointing in the intended CD. As shown in Fig. 2(a), the green and blue colors dominate the image. The absence of the red color indicates that (0001) is not lying in the CD. This is verified by the direct pole figure of {0001} in Fig. 2(c). In Fig. 2(c) there are three major texture components, which almost parallel the radial direction (RD) of the specimen and rotate towards the normal direction (ND) (in the centre of the pole figure), and the strongest one is 12.03. They result in the three maxima located on the vertical line of the $\{10\bar{1}0\}$ pole figure. From the above, the original texture can be described as a $\{10\bar{1}0\}$ fiber texture with respect to CD.

3.2 Compression test

Figure 3 shows the flow curves of Ti6Al4V under different deformation conditions, which show a typical

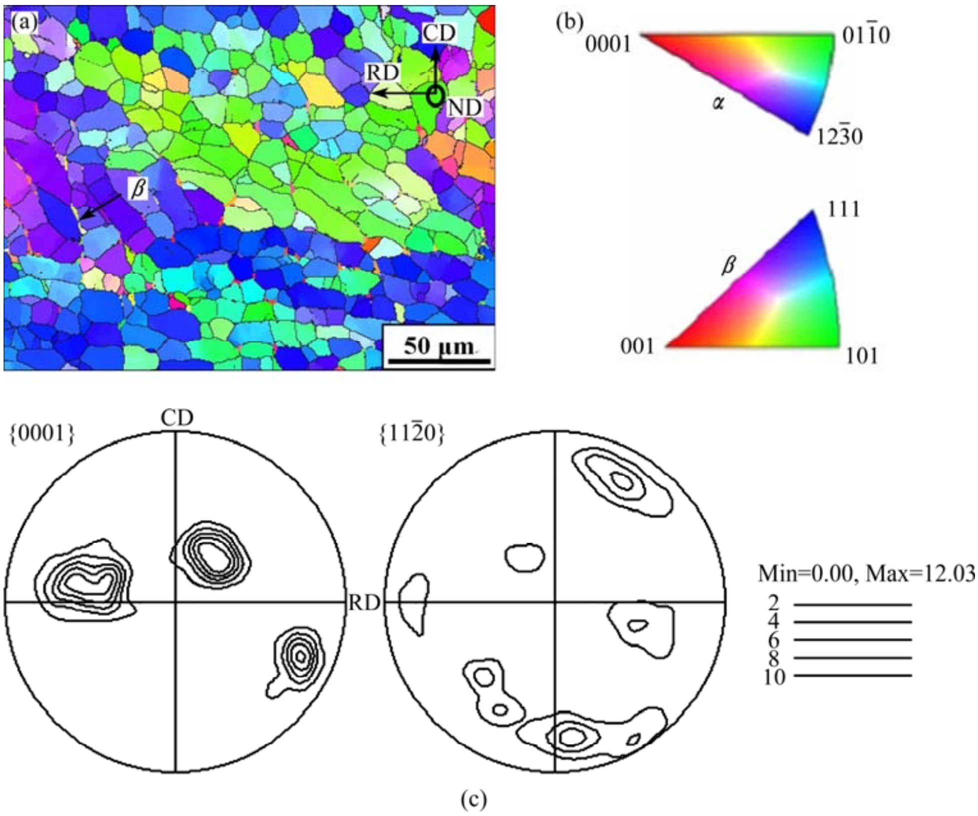

Fig. 2 Microstructure and texture of as-received Ti6Al4V revealed by EBSD maps: (a) Microstructure; (b) Orientation keys for α (HCP) and β (BCC); (c) {0001} and $\{11\bar{2}0\}$ pole figures

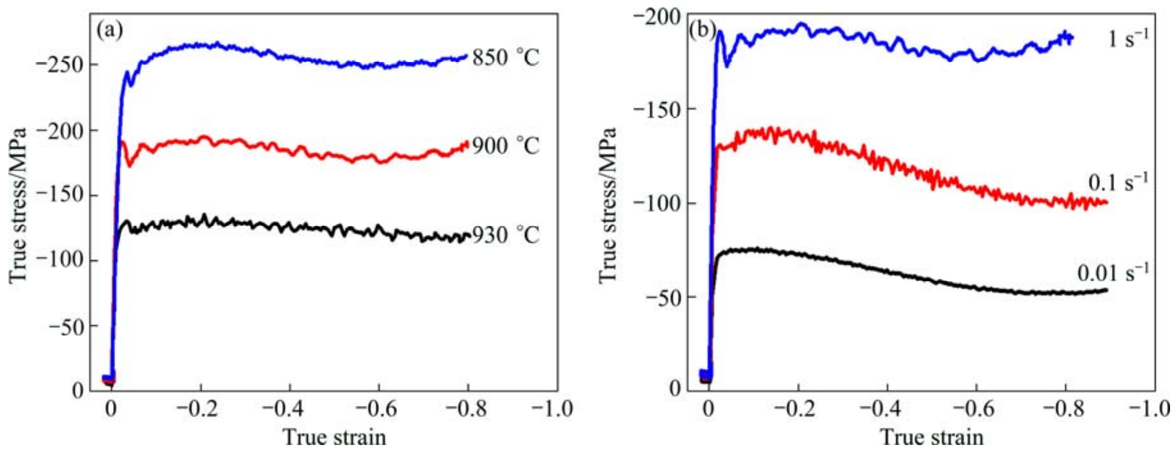

Fig. 3 True stress and true strain curves of Ti6Al4V alloy deformed under different conditions: (a) At different temperatures with same strain rate of 1 s^{-1}; (b) With different strain rate at 900 °C

dynamic recrystallization phenomenon. Figure 3(a) shows the flow curves of the specimens deformed at different temperatures with fixed strain rate of 1 s^{-1}. As the temperature increases, the peaks of flow stress curves sharply decrease, which is mainly caused by high temperature softening. The flow stress at 900 °C decreasing faster after a peak compared with that at 850 °C demonstrates that dynamic recrystallization softening becomes severe with temperature increasing. While at 930 °C much α phase transforms to β phase. As β phase is softer than α phase, it is easier for dynamic recrystallization softening and strain hardening to reach dynamic equilibrium. The curves of the specimens deformed with strain rates of 0.01, 0.1 and 1 s^{-1} at 900 °C exhibit softening after the sharp peaks (Fig. 3(b)), and the curve of strain rate of 0.1 s^{-1} decreases more severely compared with those of 1 and 0.01 s^{-1}. This is probably because at high strain rate of 1 s^{-1}, there is no enough time for dynamic recrystallization softening to occur, and for the slower strain rate of 0.01 s^{-1}, dynamic recrystallization softening becomes more prevalent. The results reveal that at low temperature with high strain rate, the deformation mechanism may be different from that at high temperature with slow strain rate.

3.3 Microstructure after deformation

Figures 4(a)−(c) show the optical metallographs at different positions of Ti6Al4V specimen deformed at 900 °C with strain rate of 1 s^{-1}. It can be seen that grains are elongated due to deformation. Furthermore, Fig. 4(c) shows that grain boundaries of the centre area become obscure. Figure 4(d) shows the macroscopic image. Figure 4(e) shows the SEM image of the centre area.

Figure 5 shows the EBSD images of the specimens under different deformation conditions. The investigated areas are all taken from the central part of the specimens subjected to the largest amount of deformation. It can be seen that dynamically recrystallized nucleation takes place preferentially at regions among elongated α grains (marked by white arrows in Figs. 5(a), (b), (d) and (e)). These fine dynamically recrystallized grains can promote boundary movement and grain rotation during the deformation. The deformation temperature is known to influence the recrystallization kinetics, as it affects the stored energy. The stored energy is regarded as a driving force for recrystallization. Deformation at a high temperature reduces the stored energy due to dynamic recovery, which retards the subsequent recrystallization. This viewpoint has been supported by numerous experimental observations of various aluminum alloys [12−15]. However, Figs. 5(a−c) show that the degree of dynamic recrystallization increases with increasing temperature. Because the strain rate is relatively high, and there is no enough time to release deformation energy, the grain deformation energy is high. Figure 5(f) shows the SEM image of a specimen deformed at 930 °C with strain rate of 1 s^{-1}. It reveals that at 930 °C dynamic recrystallization has basically completed. After deformation at 930 °C, most α phase transforms into β phase. Then the β phase transforms into needle-like α phase by fast cooling (Fig. 5(f)). Specifically, the needle-like α in Fig. 5(c) exhibits typically wavy grain boundaries. This kind of boundary is similar to the characteristic microstructure obtained from hot rolling, as reported by CHUN and HWANG et al [16]. Figure 5 shows the microstructure evolution according to strain rate. There is no perceptible influence of the strain rate on α grain, which was also reported on Ti-5-5-5-3 alloy [17]. But the degree of dynamic recrystallization increases as strain rate decreases.

Based on the above mentioned analysis, the deformation mechanism can be concluded that when temperature is below 900 °C and strain rate is higher than 0.1 s^{-1}, the microstructure is mainly composed of elongated α grains. While being deformed at 900 °C with strain rate of 0.01 s^{-1} and at 930 °C with strain rate of

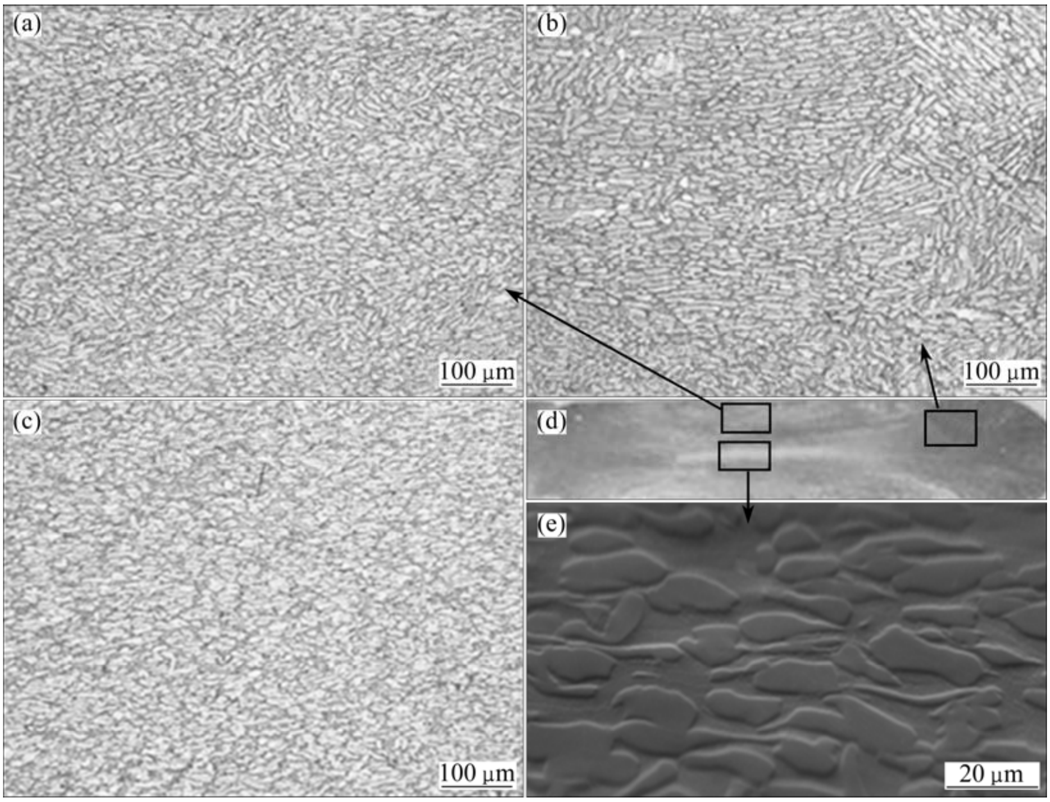

Fig. 4 Optical metallographs (a−d) and SEM image (e) of Ti6Al4V deformed at 900 °C, 1 s^{-1}

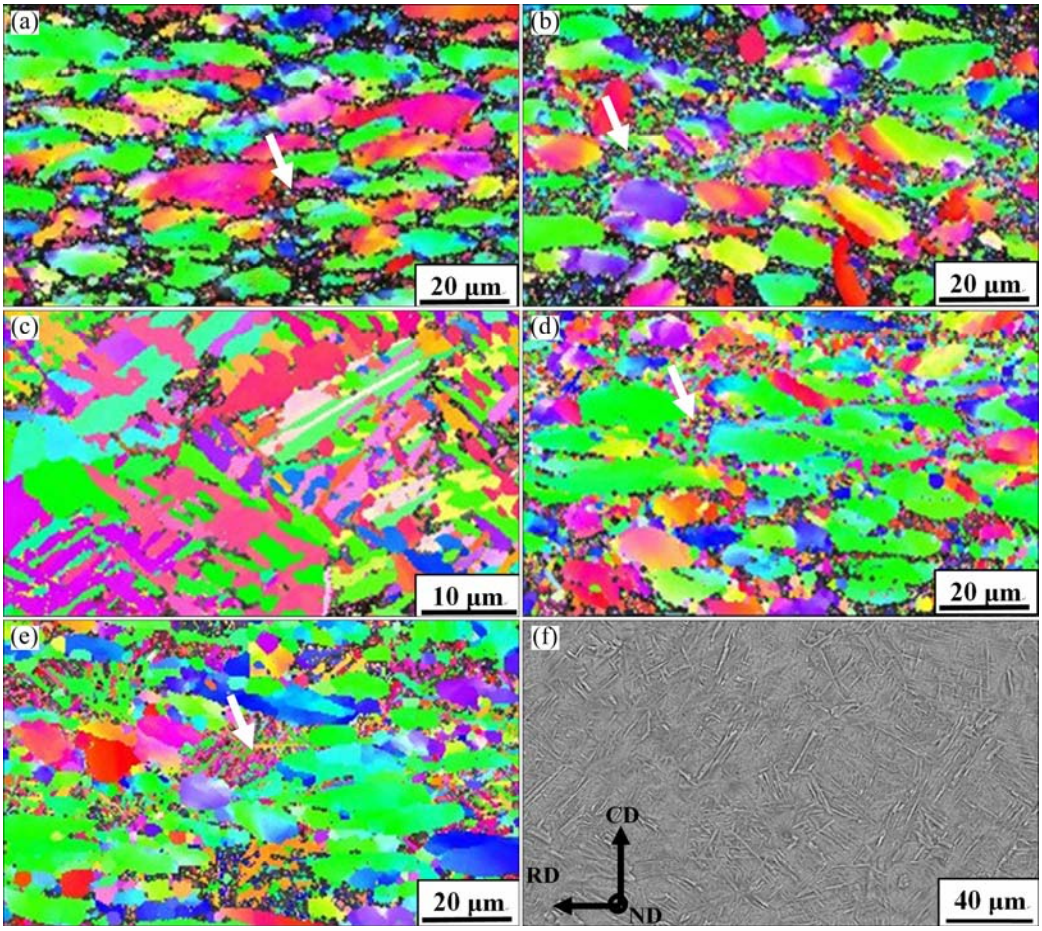

Fig. 5 EBSD maps (a−e) and SEM image (f) showing microstructure evolution of Ti6Al4V deformed under different conditions: (a) 850 °C, 1 s^{-1}; (b) 900 °C, 1 s^{-1}; (c) 930 °C, 1 s^{-1}; (d) 900 °C, 0.1 s^{-1}; (e) 900 °C, 0.01 s^{-1}; (f) 930 °C, 1 s^{-1}

1 s^{-1}, it is easier for dynamic recrystallization to take place. This can also be confirmed by the decreased LAGBs.

Figure 6 shows the distribution of grain boundaries misorientation on band contrast images. Blue lines correspond to HAGBs. LAGBs are represented with red lines. It can be seen that the LAGBs mainly appear in the elongated α grains (the gray blocks). It is known that, at first deformation makes dislocations increase and interact, and dynamic recovery makes dislocation re-array, leading to LAGBs formation and increasing, as shown by red lines in Figs. 6(a) and (b). Then LAGBs absorb dislocations, increasing grain boundaries misorientation angle. Finally, HAGBs appear due to the formation of new recrystallization grains (Fig. 6(c)). Thus, the fraction of LAGBs or HAGBs can reveal the degree of dynamic recrystallization.

Figure 7(a) shows the LAGBs fraction of the Ti6Al4V deformed at different temperatures with strain rate of 1 s^{-1} and Fig. 7(b) shows those deformed with different strain rates at 900 °C. It should be pointed out that there exists low sensitivity of the misorientation angles obtained by EBSD [18], which means that the misorientation distribution should be regarded with comparative results for different deformation conditions. As shown in Fig. 7(a), the LAGBs fraction decreases as temperature increasing. When temperature reaches 930 °C, the fraction nearly becomes zero (0.04). And the fraction increases with increasing strain rate as shown in Fig. 7(b). This is because high temperature and low strain rate can provide enough energy and time for LAGBs to transit into HAGBs [19].

Figure 7(c) shows the distribution of HAGBs of the alloy under different deformation conditions, and they reach peaks at 30°, 60° and 90°. Obviously, it is related to the phase transformation of β to α, which follows a specific orientation during cooling. The maximum peaks appear in the specimen deformed at 930 °C, 1 s^{-1}. This phenomenon will be discussed in the following part in detail.

3.4 Influence of deformation patterns on texture

The texture evolution of Ti6Al4V deformed under different conditions are shown in Fig. 8. The Ti6Al4V

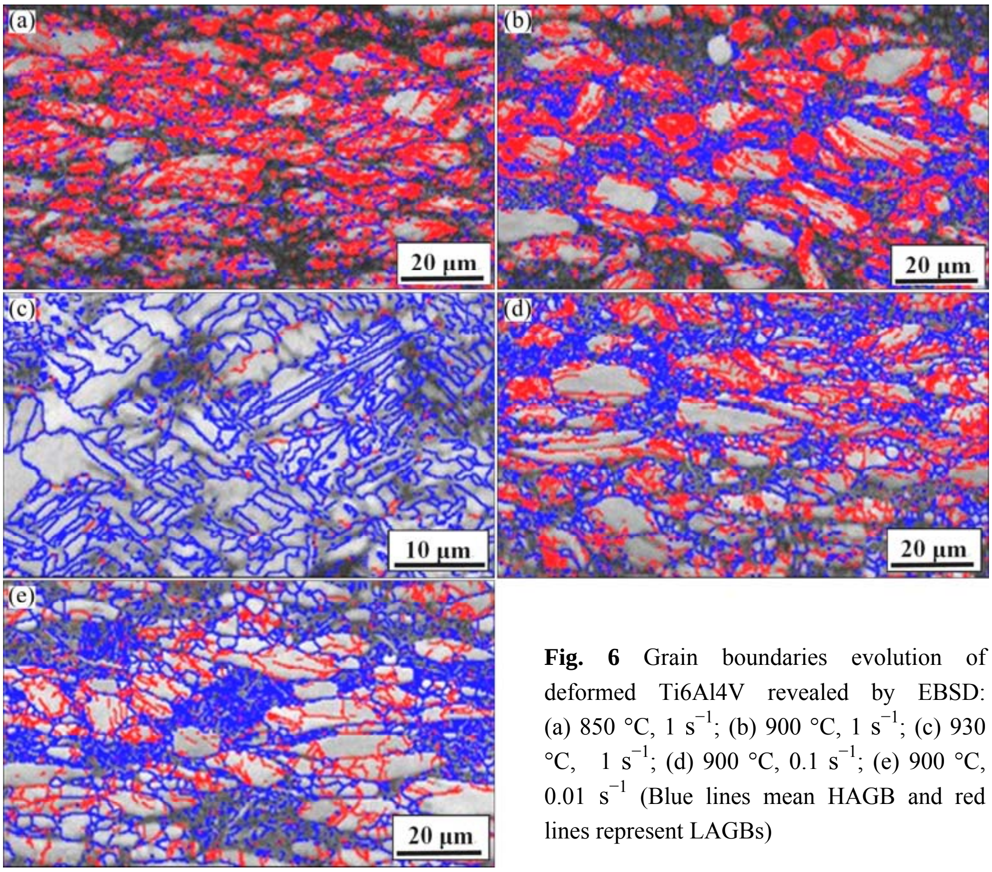

Fig. 6 Grain boundaries evolution of deformed Ti6Al4V revealed by EBSD: (a) 850 °C, 1 s^{-1}; (b) 900 °C, 1 s^{-1}; (c) 930 °C, 1 s^{-1}; (d) 900 °C, 0.1 s^{-1}; (e) 900 °C, 0.01 s^{-1} (Blue lines mean HAGB and red lines represent LAGBs)

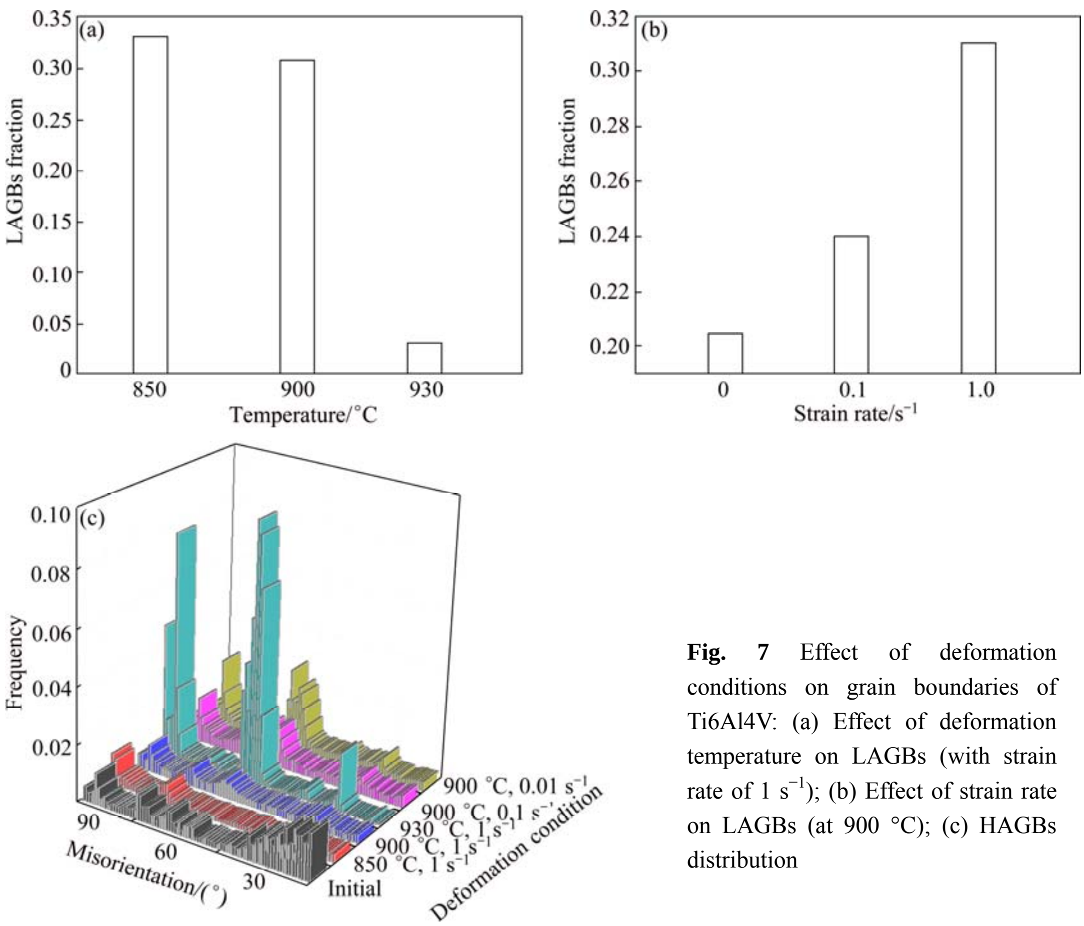

Fig. 7 Effect of deformation conditions on grain boundaries of Ti6Al4V: (a) Effect of deformation temperature on LAGBs (with strain rate of 1 s^{-1}); (b) Effect of strain rate on LAGBs (at 900 °C); (c) HAGBs distribution

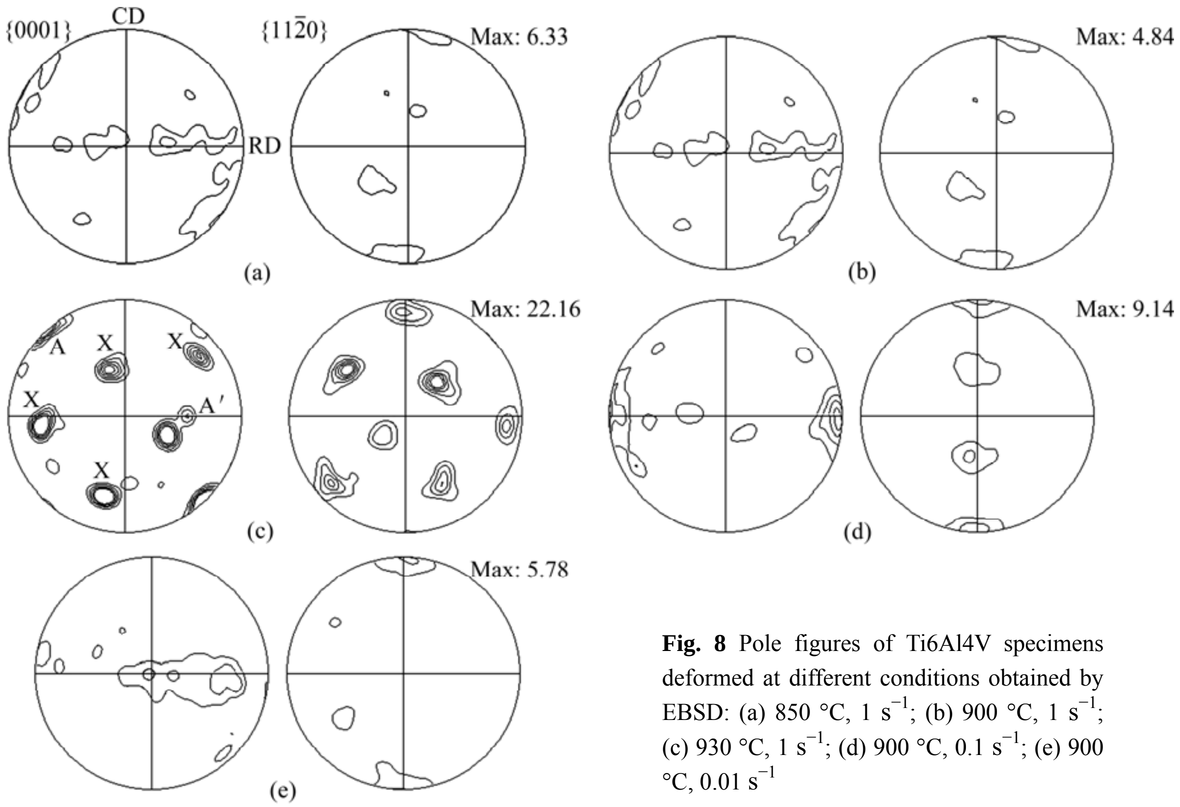

Fig. 8 Pole figures of Ti6Al4V specimens deformed at different conditions obtained by EBSD: (a) 850 °C, 1 s^{-1}; (b) 900 °C, 1 s^{-1}; (c) 930 °C, 1 s^{-1}; (d) 900 °C, 0.1 s^{-1}; (e) 900 °C, 0.01 s^{-1}

specimens deformed at 850 and 900 °C have exactly the $\{11\bar{2}0\}$ fiber texture. Figures 8(a), (b), (d) and (e) show the maxima of texture of the specimens are 6.33, 4.84, 9.14, and 5.78, respectively. Thus the textures are weaker compared with the as-received specimen (12.03, as shown in Fig. 2). This phenomenon indicates that the hot compression below 930 °C can weaken the texture of Ti6Al4V alloy with an equiaxed microstructure. The dynamic recrystallization colonies (indicated by white arrow in Fig. 5(a)) contain significant orientation rotations. With temperature increasing, the colonies enlarge. This may be the mechanism on texture weakening during deformation.

The specimen deformed at 930 °C, 1 s^{-1} (Fig. 8(c)) mostly consists of orientations marked by X, which are Burgers related to the parent β orientation, and (0002) orientations A–A'. Therefore, it takes on Burgers orientations [8]. Deformation in β phase may form a $\{110\}\langle111\rangle$ or $\{112\}\langle111\rangle$ texture [20], and β transforms to α phase following the Burgers orientation, which may form a strong transverse texture $\{10\bar{1}0\}\langle11\bar{2}0\rangle$. Thus, they confirm the Burgers orientation relationship between $(0001)_\alpha//(110)_\beta$ and $\langle11\bar{2}0\rangle_\alpha//\langle111\rangle_\beta$ [9].

Evidently as shown in Fig. 8(c), the texture (22.16) of the specimen deformed at 930 °C and strain rate of 1 s^{-1} is much stronger than that of the as-received specimen, which indicates that hot compression above 930 °C can significantly strengthen the texture of this alloy. The higher texture may be attributed to the following factors. During high temperature deformation, firstly, $\alpha\rightarrow\beta$ phase transformation forms many new orientations in new grains. Secondly, due to fast cooling β phase transforms to the lamellar microstructure (Fig. 5(c)) possessing higher texture. Finally, recrystallization of α phase can form some recrystallization texture [10].

4 Conclusions

1) The flow stress curves show typical dynamic recrystallization phenomenon. When the temperature is below 900 °C and strain rate is faster than 0.1 s^{-1}, the microstructure is mainly composed of elongated α grains. While compressing at higher temperature and lower strain rate, dynamic recrystallization takes place.

2) During high temperature deformation of Ti6Al4V alloy, dynamic recrystallization preferential nucleation occurs in the regions between elongated α grains.

3) When increasing temperature and decreasing strain rate during hot compression, LAGBs form firstly; then grain boundaries misorientation angle increases by LAGBs absorbing dislocations; finally, HAGBs appear, forming newly recrystallization grains.

4) The Burgers orientation relationship exists in the specimen hot compressed under the condition of temperature 930 °C, strain rate 1 s^{-1}, strain 70%. The texture is stronger in the specimen deformed at 930 °C

and weaker in the specimen deformed below 930 °C, compared with the as-received specimen.

References

[1] OBASI G C, BIROSCA S, PRAKASH L D G, da FONSECA J Q, PREUSS M. The influence of rolling temperature on texture evolution and variant selection during $\alpha\rightarrow\beta\rightarrow\alpha$ phase transformation in Ti−6Al−4V [J]. Acta Mater, 2012, 60(17): 6013−6024.

[2] DONACHIE M J. Titanium: A technical guide [M]. Materials Park: ASM International, 2000: 22.

[3] LUTJERING G, WILLIAMS J C. Titanium [M]. Berlin, Heidelberg: Springer, 2003: 178.

[4] YOO M H. Slip, twinning, and fracture in hexagonal close-packed metals [J]. Metallurgical Transactions A, 1981, 12(3): 409−418.

[5] CHRISTIAN J W, MAHAJAN S. Deformation twinning [J]. Progress in Materials Science, 1995, 39(1−2): 1−157.

[6] DUNST D, MECKING H. Analysis of experimental and theoretical rolling textures of two-phase titanium alloys [J]. Zeitschrift Fuer Metallkunde, 1996, 87(6): 498−507.

[7] LUO Jiao, LI Miao-quan, YU Wei-xin. Microstructure evolution during high temperature deformation of Ti−6Al−4V alloy [J]. Rare Metal Materials and Engineering, 2010, 39(8): 1323−1328.

[8] WARWICK J L W, JONES N G, BANTOUNAS I, PREUSS M, DYE D. In situ observation of texture and microstructure evolution during rolling and globularization of Ti−6Al−4V [J]. Acta Materialia, 2013, 61(5): 1603−1615.

[9] KARADGE M, PREUSS M, LOVELLB C, WITHERS P J, BRAY S. Texture development in Ti−6Al−4V linear friction welds [J]. Materials Science and Engineering A, 2007, 459(1−2): 182−191.

[10] HUANG L J, GENG L, LI A B, CUI X P, LI H Z, WANG G S. Characteristics of hot compression behavior of Ti−6.5Al−3.5Mo−1.5Zr−0.3Si alloy with an equiaxed microstructure [J]. Materials Science and Engineering A, 2009, 505(1−2): 136−143.

[11] ZENG Z P, JONSSON S, ROVEN H J. The effects of deformation conditions on microstructure and texture of commercially pure Ti [J]. Acta Materialia, 2009, 57(19): 5822−5833.

[12] GUTIERREZ I, CASTRO F R, URCOLA J J, FUENTES M. Static recrystallization kinetics of commercial purity aluminium after hot deformation within the steady state regime [J]. Materials Science and Engineering A, 1988, 102(1): 77−84.

[13] McQUEEN H J, RYUM N. Hot working and subsequent static recrystallization of Al and Al−Mg-alloys [J]. Scandinavian Journal of Metallurgy, 1985, 14(4): 183−194.

[14] RAGHUNATHAN N, ZAIDI M A, SHEPPARD T. Recrystallization kinetics of Al−Mg alloys AA5056 and AA5083 after hot deformation [J]. Materials Science and Technology, 1986, 2(9): 938−945.

[15] VANDERMEER R A, JENSEN D J. Recrystallization in hot vs cold deformed commercial aluminum: A microstructure path comparison [J]. Acta Materialia, 2003, 51(10): 3005−3018.

[16] CHUN Y B, HWANG S K. Static recrystallization of warm-rolled pure Ti influenced by microstructural inhomogeneity [J]. Acta Materialia, 2008, 56(3): 369−379.

[17] JONES N G, DASHWOOD R J, DYE D, JACKSON M. Thermomechanical processing of Ti−5Al−5Mo−5V−3Cr [J]. Materials Science and Engineering A, 2008, 490(1−2): 369−377.

[18] CABIBBO M, BLUM W, EVANGELISTA E, KASSNER M, MEYERS M. Transmission electron microscopy study of strain-induced low- and high-angle boundary development in equal-channel angular-pressed commercially pure aluminum [J]. Metallurgical Transactions A, 2008, 39(1): 181−189.

[19] LI H Z, LI Z, ZANG W, WANG Y, LIU Y, WANG H J. High temperature deformability and microstructural evolution of Ti−47Al−2Cr−0.2Mo alloy [J]. Journal of Alloys and Compounds, 2010, 508(2): 359−363.

[20] GEY N, HUMBERY M. Characterization of the variant selection occurring during the $\alpha\rightarrow\beta\rightarrow\alpha$ phase transformations of a cold rolled titanium sheet [J]. Acta Materialia, 2002, 50(2): 277−287.

Ti6Al4V 钛合金的变形组织及织构

杨柳青，杨延清

西北工业大学 材料学院，凝固技术国家重点实验室，西安 710072

摘 要：在温度 850~930 °C、应变速率 0.01~1 s^{-1} 的条件下，对初始组织为等轴组织的 Ti6Al4V 钛合金进行变形程度为 70%的热压缩变形实验，研究合金的变形组织及织构。结果表明，当温度低于 900 °C、应变速率高于 0.1 s^{-1} 时，合金的组织主要是拉长的 α 晶粒；而在高于 900 °C 以及低应变速率下，则会发生动态再结晶。电子背散射衍射(EBSD)结果显示，合金在再结晶过程中亚晶界吸收位错，最终形成大角晶界。在 930 °C 时动态再结晶已基本完成，水冷至室温时形成针状 α 相。与原始组织相比，合金在 930 °C 变形时织构得到增强，低于 930 °C 变形时织构变弱。

关键词：Ti6Al4V 合金；热压缩；动态再结晶；EBSD；织构

(Edited by Hua YANG)